J Mater Sci: Mater Electron (2021) 32:18212–18223

The variations of electrical resistivity and thermal conductivity with growth rate for the Zn–Al–Cu eutectic alloy

Necmettin Maraşlı[1,*], Ümit Bayram[2], and Sezen Aksöz[3]

[1] Department of Mechanical Engineering, Faculty of Engineering, İstanbul Aydın University, 34294 İstanbul, Turkey
[2] Central Research Facility (AGU-CRF), Abdullah Gül University, 38080 Kayseri, Turkey
[3] Department of Physics, Nevşehir Hacı Bektaş Veli University, 50300 Nevşehir, Turkey

Received: 30 April 2021
Accepted: 7 June 2021
Published online: 24 June 2021

ABSTRACT

The Zn–Al–Cu alloy (Zn–5wt%Al–0.5wt%Cu) is solidified with different growth rates (V = 8.45–2087.15 μm s^{-1}) at a constant temperature gradient (G = 3.67 K mm^{-1}) using Bridgman-type directional solidification apparatus (BTDSA). The thermal conductivity (K) and electrical resistivity (ρ) for the Zn–Al–Cu alloy solidified with the different V values are measured by the longitudinal heat flow method (LHFM) and DC four-point probe technique (FPPT), respectively. The λ and K decrease with the increasing V, while the ρ increases with increasing V in the Zn–Al–Cu eutectic alloy. The dependences of ρ and K on λ and V for the Zn–Al–Cu eutectic alloy are obtained as $\rho = 9.98 \times 10^{-8}\lambda^{-0.18}$, $\rho = 7.03 \times 10^{-8}V^{0.07}$, $K = 110.91\lambda^{0.104}$ and $K = 144.59V^{-0.040}$, respectively. The melting enthalpy (ΔH_f) and specific heat difference between solid and liquid phases (ΔC_p) for the Zn–Al–Cu eutectic alloy are determined as 113.89 J g^{-1} and 0.172 J g^{-1} K^{-1}, respectively, by the differential scanning calorimetry (DSC).

1 Introduction

Biomedical materials are used to fulfil the functions of living tissues in the human body or contribute to their treatment. Biomedical materials are very special materials that should be highly compatible with the living tissue where they are implanted and not have any toxic effects. The mechanical and physical properties of available permanent implants must have high potential to meet the functions of the area where it is applied. The only way to overcome the expected mechanical strength is to use metal alloys, but the alternative materials have been produced in very limited numbers yet [1–5]. However, metal alloys carry the risk of releasing particles that can cause carcinogenic, toxic or allergic side effects into the biological environment through wear or corrosion [6–9]. In addition, problems such as growth restriction of the body and obstacles in medical imaging in paediatric applications caused difficulties for using permanent implants so it is necessary to develop biodegradable materials to replace them.

Address correspondence to E-mail: nmarasli65@gmail.com

https://doi.org/10.1007/s10854-021-06363-x

Zinc like magnesium is useful body elements in many biological processes in human organism [10–12]. Recently, Zn-based binary or multicomponent alloys have attracted attention for their biodegradability and adaptability to tissue regeneration. Aluminium is a neurotoxin element and causes cognitive deficiency [13, 14]. Recently, Bowen et al. [15] have reported that Zn–X wt% Al (X = 1–5) alloys can be used for stent applications.

Zn-based Zn–Al alloys have good strengths and hardness and show good wear resistant when it is compared with pure zinc or pure aluminium [16]. Zn–Al-based ternary or multicomponent alloys have been developed for their high performance and high-quality die-castings in automotive industry [17]. Copper is also added as alloying element into the Zn–Al alloys to improve mechanical and corrosion performances [18–21].

Since the solidification stage affects many properties of metallic materials, it is undoubtedly the most important stage in their production [22–26]. The main characteristics of the material are determined by the controlling of solidification parameters, which are the temperature gradient (G), growth rate (V) and alloy composition (X). The cooling rate ($T' = dT/dt = V \times G$) is an effective control parameter for directionally solidification of alloys [27–31] and the microstructural, mechanical and physical properties of directionally solidified alloys depend on V.

The Zn-based biodegradable materials have lower thermal and electrical conductivity in comparison with magnesium and the dependences of their electrical and thermal properties on solidification stage should be investigated. The ρ and K values of alloys are fundamental physical parameters to control the performance and depend on V as well as the T and X. In the literature, although a lot of researches were mainly focussed on the directionally solidification of alloys to determine the dependence of microstructure parameters (primary dendrite arm spacing λ_1, secondary dendrite arm spacing λ_2 and eutectic spacing λ) and mechanical properties (hardness, HV and ultimate tensile strength, σ_{UTS}) on V [28–44]. In addition, the variations of K and ρ with T for alloys were also investigated [45–47]. The results from the previous studies show that there are significant data show the dependence of λ_1, λ_2, λ HV and σ_{UTS} on V or K and ρ on T, especially a few studies present to show that the dependence of K on V for alloys [48]. Recently, the variation of K with V for the Al–Cu–Ni eutectic system was determined [48]. Based on the work [48], the effects of V on ρ and K are aimed to be investigate for the Zn–Al–Cu eutectic alloy.

2 Experimental procedures

It is known that changes in the microstructure of materials (particle sizes) affect their mechanical properties (such as microhardness and stress) and other properties (such as electrical conductivity, thermal properties and corrosion). The formation of regular microstructures and particle sizes (λ) in the materials depend on G, V and X during the solidification of these materials. In other words, by controlling G, V and X independently from each other, it is possible to influence the microstructures, mechanical, electrical and thermal properties of the materials with the directional solidification method.

Based on this information, the experimental processes for the Zn–Al–Cu alloy consist of alloy solidification with the different V, determination of G, V and λ and the measurements of ρ and K. These processes are outlined as fallows.

2.1 Directional solidification of the Zn–Al–Cu alloy

The solid solubility of solid Cu in the solid Zn is 2.75 wt% Cu. Therefore, Cu was added into Zn–5 wt% Al to be 0.5 wt% Cu to growth the η-Zn and the β-eutectoid phases from the Zn–Al–Cu eutectic liquid. The hot filling furnace is heated up to 700 K while the sufficient amount of 4 N and 3 N purity of Zn, Al and Cu, respectively, were melted under vacuum. After homogenization, the molten Zn–Al–Cu was poured into graphite pots which are held in a hot filling furnace and then solidified upward to get full fill the specimens.

Each specimen was then re-melted at 800 K in a BTDSA as shown in Fig. 1. After achieving thermal stabilization, the molten alloy was solidified as 10 or 15 cm by pulling it downwards with a constant pulling speed and then rapidly quenched into the cold water bath [38–43]. The highest V value of 2087.15 μm s^{-1} was achieved with a driving system specially constructed in the present work. The directional solidifications of Zn–Al–Cu with the

different V (from 8.45to 2087.15 μm s^{-1}) were done at 3.67 K mm^{-1} by using the driving system.

2.2 Measurements of G, V and λ

0.25 mm thick and metal sheathed K–type thermocouples were used to measure the temperature difference (ΔT) within a known space of ΔX = 4–5 mm) into the sample. All the thermocouple ends were connected to a data logger via computer and thus, the data logger recorded the cooling rate during the growth. The time required for the solid–liquid interface passes the distance between a thermocouple pairs (Δt) were read from data-logger record. Thus, the value of $V = \Delta X/\Delta t$ and $G = \Delta T/\Delta X$ for each sample was determined from the ΔT, Δt and ΔX.

Some routine metallographic processes were carried out to reveal the microstructure of samples. For these metallographic processes, the transverse sections of samples, cut in a length of 15 mm were flatted, cold mounted and then polished. After polishing, the samples were etched with a 10% HF in water enchant for 40–45 s.

Typical SEM photographs of microstructures for the Zn–Al–Cu alloy solidified with the different V are shown in Fig. 2. The microstructure of the Zn–Al–Cu is the lamellar eutectic structure, and has fine lamellar with increasing V.

The λ values measured from microstructure photographs taken from the transverse sections by the linear intersection method [38]. In the measurement of λ, 30–40 λ measurements for each V were done to increase the statistical reliability. Hence, the statistical error in the measurements of the microstructures was minimized, and it is given in Table 1.

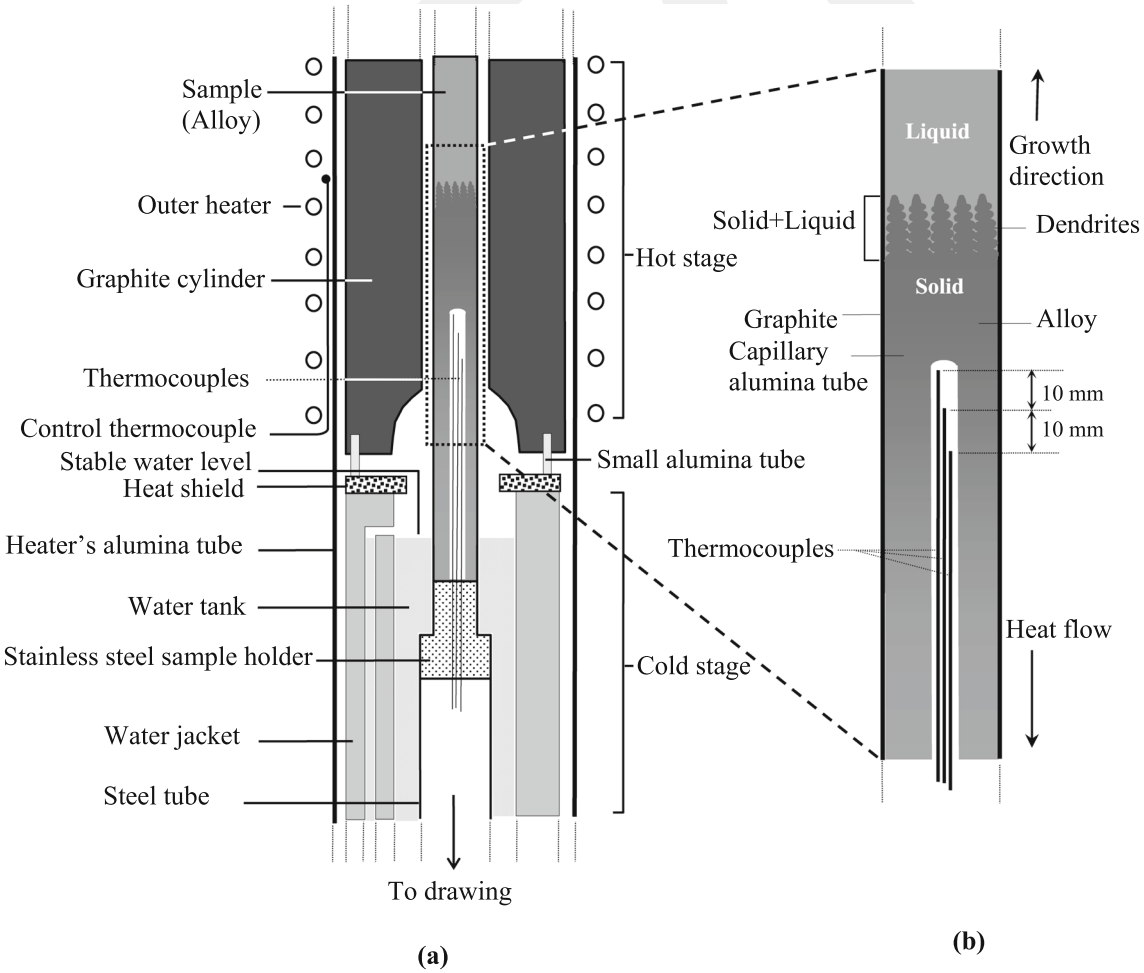

Fig. 1 Schematic illustration of the BTDSA: **a** Hot and cold stages and **b** the sample details

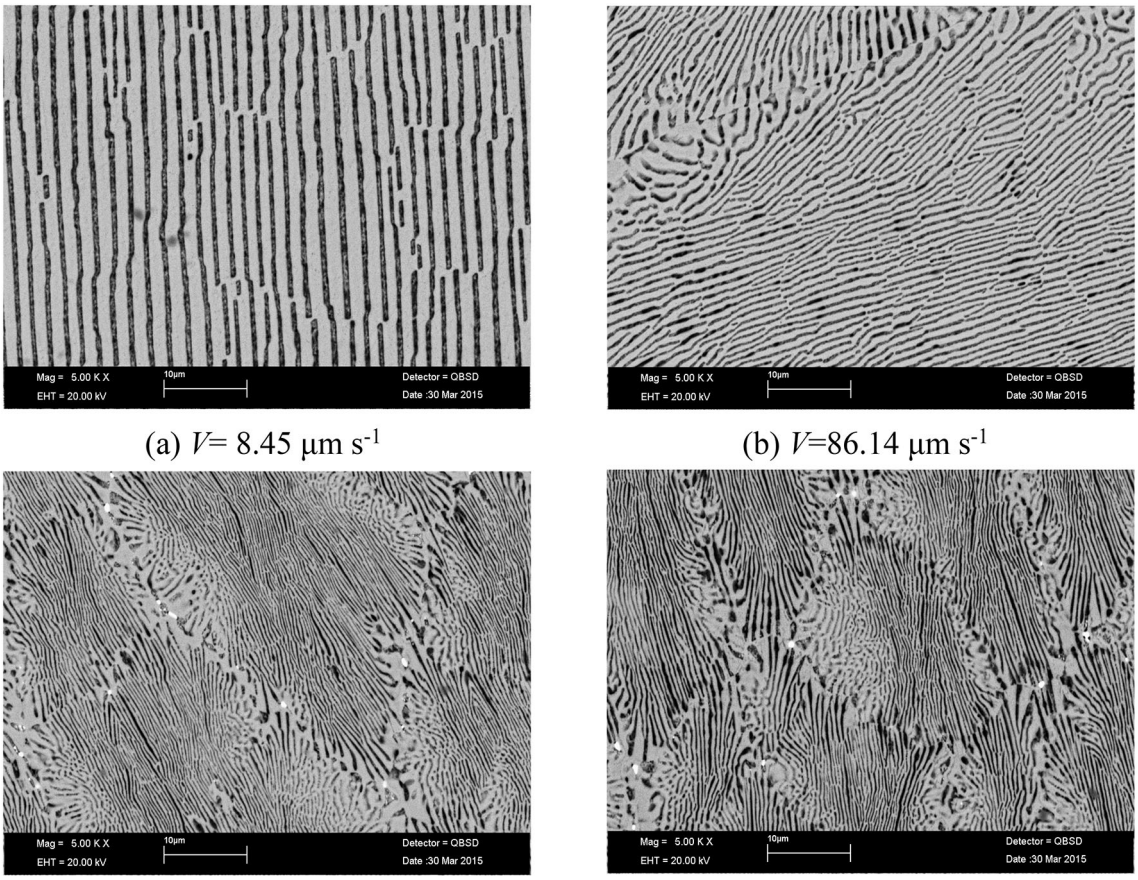

Fig. 2 Typical SEM images for Zn-5 wt% Al-0.5 wt% Cu alloy directionally solidified with different V at 3.67 K mm^{-1}

Table 1 The solidification parameters, eutectic spacing, electrical resistivity and thermal conductivity for directional solidified Zn-5 wt% Al-0.5 wt% Cu eutectic alloy

Alloy (wt%)	G (K mm^{-1})	V (μm s^{-1})	λ_E (μm)	$\rho \times 10^{-8}$ (Ω m)	K (W m^{-1}K^{-1})
Zn–5Al–0.5Cu	3.67	8.45	3.35	8.36	139.49
		41.32	1.67	8.89	133.97
		86.14	1.18	9.63	129.66
		166.58	0.81	9.96	124.92
		465.36	0.61	10.62	122.05
		1032.47	0.52	10.98	118.36
		1544.62	0.45	11.82	114.89
		2087.15	0.39	12.43	110.23

2.3 Measurements of ρ

The ρ is the basic fundamental physical property of materials such as thermal resistivity, thermal expansion coefficient, melting point, specific heat, and bulk module. In literature, many works on ρ measurements for pure metals are present, but the studies on determination of ρ for multicomponent systems are very limited. In alloys, the ρ depends on temperature, dimension of phases and grain size, plastic deformation, annealing conditions and composition of alloy [49].

The ρ values for the directionally solidified Zn–Al–Cu alloy with different V values were measured by DC FPPT [49]. In the measurement of ρ [50–52], the constant DC potential voltage is applied on the

specimen and the current (I) and potential difference on the specimen (ΔV) are measured by ampere meter and volt meter, respectively. The dimension of the road sample was 4 mm in diameter and 30 mm in length and the space between the probes was 1 mm.

The ρ is expressed as

$$\rho = RCF\frac{\Delta V_{measured}}{I_{measured}} \quad (1)$$

where RCF is the resistivity correction factor which is calculated to be 0.364 cm for the sample [43, 44].

The ρ measurements for the disc samples were conducted at 300 K. The measuring unit was interfaced with a computer for the online data acquisition and processing. Keithley 2400 DC power supply and 2700 multimeter were used to measure the current and the potential drop, respectively. The probes are made of 0.5-mm thick platinum wire and the ρ was determined from Eq. 1 using the measured values of I and ΔV.

The experimental error in the ρ measurements is about 5% [51].

2.4 Measurements of K

The K is the basic thermal property of materials. Although the value of K for pure metals was determined from theoretical approaches and experimental studies, the sufficient information or available data on K value for alloys are not exist. The K for alloy change with T and V as well as composition of alloy, X.

The LHFM is useful technique to determine K value for solid materials. In this technique, an experimental system is used to get a longitudinal heat flow thorough to the cylindrical sample. Assuming heat flow is steady state and no radial heat loss or gain, K is determined from one-dimensional heat conduction by Fourier–Biot law [53, 54];

$$K = \frac{\overset{*}{Q}\Delta X}{A\Delta T} \quad (2)$$

where $\overset{*}{Q}$ is the heat flow rate, A is the surface area which is normal to heat flow direction and $\Delta T = T_1 - T_2$ is the temperature difference read by a thermocouple pair and $\Delta X = X_1 - X_2$ is the distance between thermocouple pairs positions.

In the present work, an LHF apparatus [55, 56] was used to determine the K for the Zn–Al–Cu alloy solidified with the different V at 300 K. The solidified cylindrical sample was cut 30 mm in length which consists of two zones; 20 mm length of sample contains one end closed alumina tube and 10 mm length other part of sample does not contain alumina tube. The cylindrical specimen of 30 mm length was then placed into the LHF apparatus. The sample was kept at a constant temperature gradient by heating one side of sample by a hot stage and cooling the other side of sample by a cold stage. The temperature of heater and cold stages were hold at 300 K and 253 K, respectively, with a PID temperature controller. The side surface of sample was wrapped with glass fibre blanket to get the LHF through to the cylindrical specimen and stop the radial heat loss from the specimen. 10 mm space between the hot stage and cold stage was set. The samples were kept under steady state heat flow conditions at least 4 h and the values of ΔT, I and ΔV_{heater} were recorded with a data logger and the data acoustics via to computer, respectively for sensitive K measurements. The values of K were calculated from Eq. 2 using the measured values of $A, \overset{*}{Q} = I \times \Delta V_{\text{heater}}$, ΔT and ΔX.

2.5 Determinations of ΔC_p and ΔH_f

The sample was heated up to 1000 K with a heating rate of 10 K/min using a DSC to determine the ΔC_p and ΔH values for the Zn–Al–Cu alloy. The ΔC_p is expressed as

$$\Delta C_p = \frac{\Delta H_f}{T_m} \quad (3)$$

where T_M is the alloy melting temperature. Thus, ΔH_f is determined from DSC trace by determining the area under the peak and the ΔC_p value is calculated from Eq. 3 using the values of ΔH_f and T_m.

3 Results and discussions

3.1 Microstructure analysis

The eutectic composition of the Zn–Al–Cu alloy was identified as Zn–5wt% Al–0.5 wt% Cu [57, 58]. The composition of Cu in the Zn–Al alloy should be lower than 2.75 wt% Cu which is the maximum solid solubility of Cu in solid Al [57, 58] at 821 K. Thus, the eutectic reaction at the near the eutectic composition is that the eutectic L → η-Zn solution solid matrix (Zn–0.84wt% Al–1.78 wt% Cu) + α-Al solution (Al–

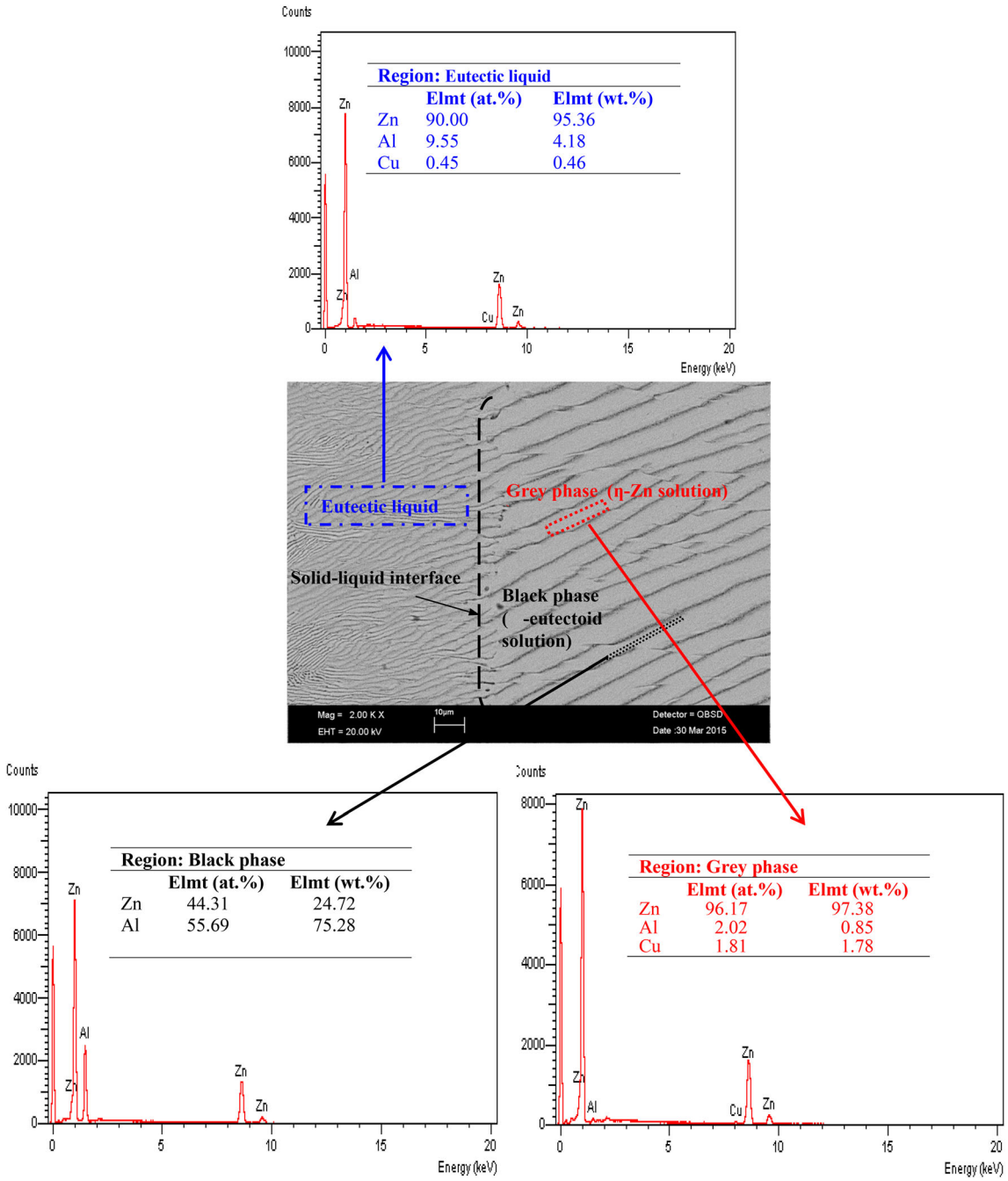

Fig. 3 The chemical composition analysis of Zn-5wt%Al-0.5wt%Cu eutectic alloy using SEM EDX. Black phase is the β-eutectoid phase and grey phase is η-Zn matrix solution phase

24.72 wt% Zn) phases [57, 58]. Thus, Zn–5 wt% Al–0.5 wt% Cu was preferred as alloy composition to growth the solid η-Zn and α-Al solutions phases from the Zn–Al–Cu eutectic liquid.

Typical SEM photographs of the Zn–Al–Cu alloy solidified with different V are given in Fig. 2. The microstructure of the Zn–Al–Cu has fine lamellar eutectic of η-Zn and α-Al phases with increasing V.

The chemical composition analyses of η-Zn and α-Al solid solutions were performed via EDX (energy-dispersive X-ray). From EDX results as shown in Fig. 3, the η-Zn and α-Al are the grey and black colours, respectively.

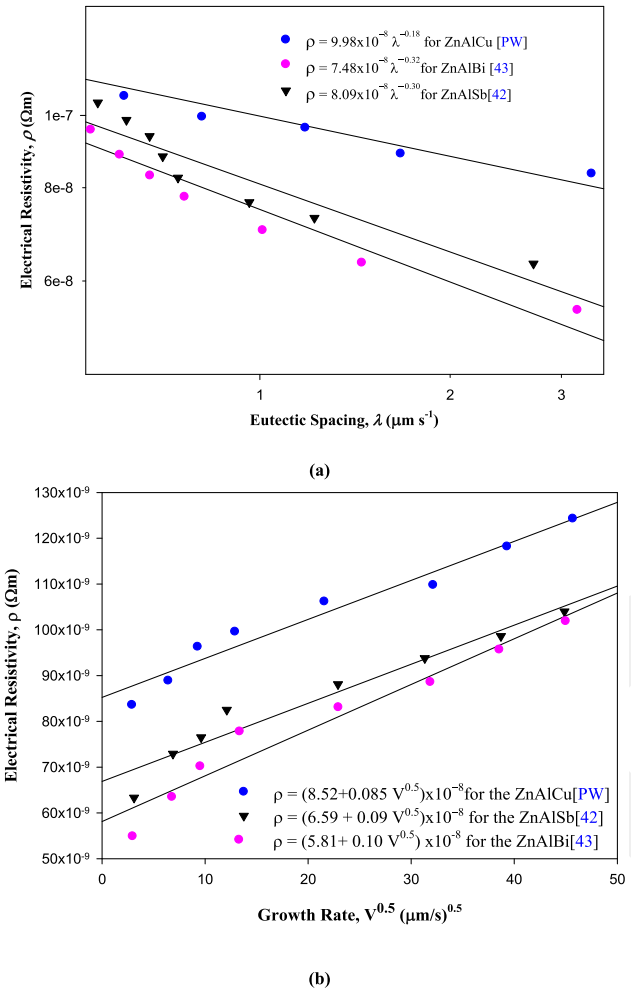

Fig. 4 The variations of ρ as a function of **a** λ and **b** V determined in the form of Hall–Petch type equation for the Zn-based ternary eutectic alloys

3.2 Dependence of ρ on λ and V

The ρ values for the Zn–Al–Cu solidified with different magnitudes of V were measured at 300 K with the FPP technique. The λ decreases with the increasing V or vice versa at 3.67 K mm^{-1} as shown in Fig. 2. The highest and lowest λ values were obtained with 8.58 μm s^{-1} and 2038.65 μm s^{-1} as shown in Fig. 2a and b, respectively. The variation of ρ with the λ and V in the form of Hall–Petch equation is plotted as shown in Fig. 4, and the relationships between them were determined as follows:

$$\rho = \left(7.89 + 1.73\,\lambda^{-1}\right) \times 10^{-8} \quad (4)$$

$$\rho = \left(8.52 + 0.085\,V^{0.5}\right) \times 10^{-8} \quad (5)$$

The dependence of ρ on λ and V were obtained in the form of Hall–Petch equation for the Zn–Al–Sb [42, 44] and Zn–Al–Bi [43, 44]. A comparison of the present results with the previous results obtained for the Zn–Al–Sb [42, 44] and Zn–Al–Bi [43, 44] is also given in Fig. 4.

Lines of ρ variations with λ and V for the Zn–Al–Cu are above the lines of ρ variations with λ and V for the Zn–Al–Sb [42, 44] and Zn–Al–Bi [43, 44]. The coefficient of 1.73 for λ in the Zn–Al–Cu is 60 percent smaller than the coefficients of 2.85 and 2.63 for λ in the Zn–Al–Sb [42, 44] and Zn–Al–Bi [43, 44], respectively, while the initial resistivity value of 7.89 for λ in the Zn–Al–Cu is 75 percent bigger than the initial values of 4.51 and 4.97 for λ in the Zn–Al–Sb [42, 44] and Zn–Al–Bi [43, 44], respectively. The coefficients of V in the Zn-based ternary alloys are very close to each other's while the initial resistivity value of 8.52 for V in the Zn–Al–Cu is about 45 percent bigger than the initial resistivity values of 5.81 and 6.59 for λ in the Zn–Al–Sb [42, 44] and Zn–Al–Bi [43, 44], respectively.

The ρ increases from 8.36×10^{-8} to 12.43×10^{-8} Ω m with increasing V from 8.45 to 2087.15 μm s^{-1} and any increment in the V leads to an increment in ρ as shown in Fig. 5 and given in Table 1 for the Zn–Al–Cu. The relationships between ρ and λ and V in logarithmic scale for Zn–Al–Cu eutectic system were also determined as:

$$\rho = 9.98 \times 10^{-8}\,\lambda^{-0.18} \quad (6)$$

$$\rho = 7.03 \times 10^{-8}\,V^{0.07} \quad (7)$$

The influences of λ and V on ρ were obtained for the Zn–Al–Sb [42, 44] and Zn–Al–Bi [43, 44]. The present results were also compared with the previous results obtained for the Zn–Al–Sb [42, 44] and Zn–Al–Bi [43, 44] in Fig. 5. The ρ variations with λ and V lines for the Zn–Al–Cu are above the ρ variations with λ and V lines for the Zn–Al–Sb [42, 44] and Zn–Al–Bi [43, 44].

The exponent value of 0.18 related with λ for the Zn–Al–Cu is about 40 percent of 30 and 32 exponent values for the Zn–Al–Sb [42] and Zn–Al–Bi [43], respectively, and the initial resistivity value of 9.98 is slightly bigger than the initial resistivity values of 8.09 and 7.48 for the Zn–Al–Sb [42] and Zn–Al–Bi [43], respectively, as can be seen from Fig. 5. The ρ versus V line for the Zn–Al–Cu is far from the ρ versus V line for the Zn–Al [41]. This difference is

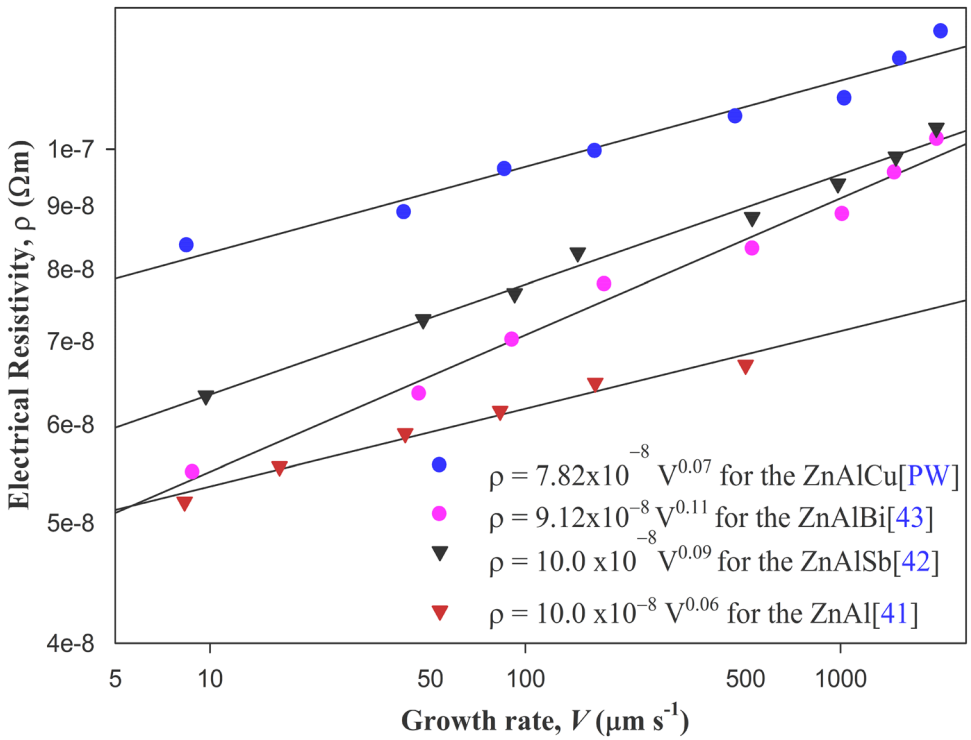

Fig. 5 The variations of ρ as a function of V determined by linear regression analysis for the Zn-based binary and ternary eutectic alloys

probably due to the microstructure difference between the Zn–Al–Cu and Zn–Al [41] because of the microstructure of the Zn–Al–Cu and Zn–Al [41] are eutectic lamellar and dendrite structures, respectively. The ρ versus V line for the Zn–Al–Cu is slightly above the ρ versus V lines for the Zn–Al–Bi [43] and Zn–Al–Sb [42]. From Fig. 5b, it can be concluded that the exponent value of 0.07 related with V for the Zn–Al–Cu is very close the exponent value of 0.06 for the Zn–Al [41], but is smaller than the exponent values of 0.09 and 0.11 related V for the Zn–Al–Sb [42] and Zn–Al–Bi [43], respectively.

The ρ value for Zn, Al, Cu, Bi and Sb are about 5.92×10^{-8},2.65×10^{-8}, 1.70×10^{-8}, 129.0×10^{-8} and 41.3×10^{-8} Ω m [59], respectively, at 300 K. If the variations of ρ with V obtained in the present work and previous works [22–24] shown in Figs. 4 and 5, respectively are considered together it can be concluded that Cu content in the Zn–Al eutectic system increases the its ρ value according to the Bi and Sb contents. This means that the hardness of Zn–Al–Cu eutectic system might be higher than the hardness of Zn–Al–Bi and Zn–Al–Sb eutectic systems and these differences in ρ values are due to alloying element types rather than growth rates.

3.3 Influence of λ and V on K

The variations of K with λ and V for the Zn–Al–Cu have been plotted in Fig. 6, and the related data are given in Table 1. As shown in Fig. 6, the K linearly increases or decreases with increasing the λ or V, respectively. The relationships between K and λ and V for the Zn–Al–Cu were expressed as follows:

$$K = 110.91\,\lambda^{0.104} \tag{8}$$

$$K = 144.59\,V^{-0.040} \tag{9}$$

As seen from Table 1 and Fig. 6, the K value of 110.23 and 139.49 W K^{-1} m^{-1} for the Zn–Al–Cu is correspond of the lowest 8.45 μm s^{-1} and highest 2087.15 μm s^{-1}, respectively at 300 K. The K values for Al, Zn, Bi and Zn-3 at.%Al-0.3 at.%Bi are 236, 119, 6.3 and 157 W K^{-1} m^{-1} [60–62], respectively, at 300 K. The highest value of 139.49 and the lowest value of 110.23 W K^{-1} m^{-1} are around the value of 119 W K^{-1} m^{-1} for pure Zn [58]. The highest value of 139.49 W K^{-1} m^{-1} is slightly higher than the value of cast Zn-based alloy measured in the previous work [61].

In the previous works [60–62], the K measurements were done for cast alloys i.e. the molten alloys into mould were solidified under transient condition, i.e.

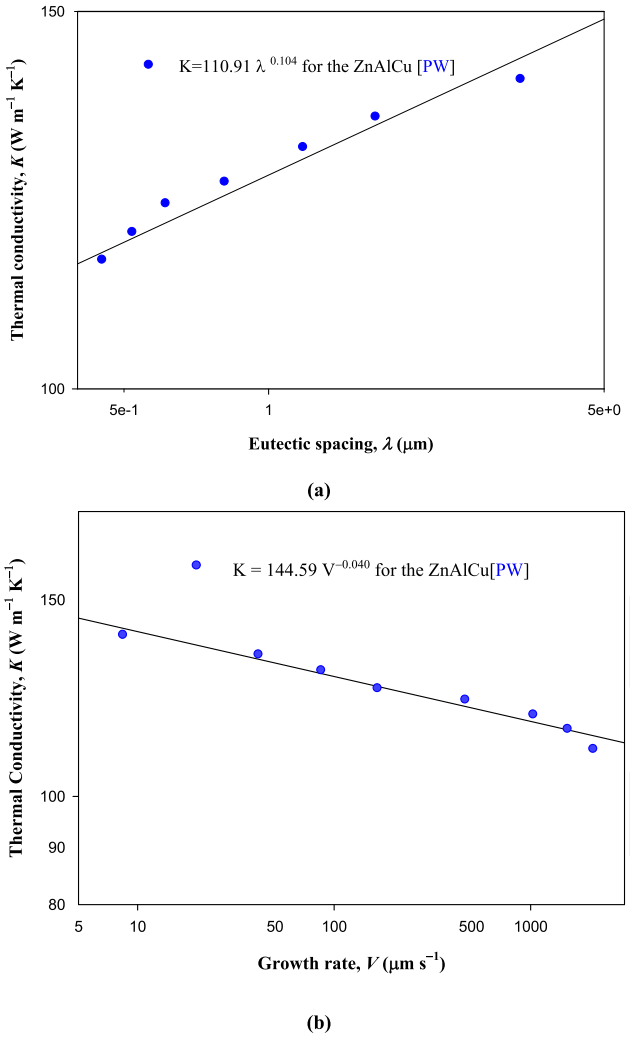

Fig. 6 The variations of K with **a** λ and **b** V for Zn-5wt%Al-0.5wt%Cu eutectic alloy

the growth rate is not constant and varies with time during the solidification. Also, the V value for cast might be higher than the highest V value for directional solidification. Therefore, the grain and phase dimensions for the cast alloys might be smaller than the grain and phase dimensions for directional solidified alloys and the microstructure of cast alloys should not be uniform and irregular or disordered while the microstructure of directionally solidified alloys for a given V are regular and uniform. Thus, the K value for directional solidified alloys for a given V should be higher than the K value for cast alloy. Therefore, the difference between the present and previous K values for the Zn–Al eutectic system might be due to the sample preparation under the different type of solidification conditions for K measurements.

3.4 Determination of ΔC_p and ΔH_f for the Zn–Al–Cu eutectic alloy

Zn–Al–Cu eutectic alloy was heated with 10 K min^{-1} up to 800 K with a DSC and the trace of heat flow versus temperature is given in Fig. 7. T_M was detected as 660.54 K and ΔH_f and ΔC_p were determined to be 113.89 J g^{-1}, and 0.172 J g^{-1} K^{-1}, respectively from the trace of heat flow versus temperature. The ΔH and ΔC_P values obtained in the present work well agree with the values 108.59 J g^{-1} and 0.165 J g^{-1} K^{-1}, 112.55 J g^{-1} and 0.291 J g^{-1} K^{-1}, 112.55 J g^{-1} and 0.309 J g^{-1} K^{-1} and 113.4 J g^{-1} and 0.294 J g^{-1} for the Zn–Al–Sb [42], Zn–Al–Bi [43], Zn–Al [40] and Zn–Al [39], respectively. The recommended values of ΔH and the ΔC_P are 396.96 J g^{-1} and 0.896 J g^{-1} K^{-1} and 111.91 J g^{-1} and 0.389 J g^{-1} K^{-1} for the Al [63] and Zn [63], respectively.

4 Conclusion

In the present work, Zn–5wt%Al–0.5wt%Cu eutectic alloy was directionally solidified with a wide range of growth rate (V = 8.45 μm s^{-1}–2087.15 μm s^{-1}) at G = 3.67 K mm^{-1} and then, the microstructure analysis and measurement of electrical resistivity (ρ) and thermal conductivity (K) were carried out for the solidified samples. The primary results obtained in this study can be listed in detail as follows:

1. After appropriate metallurgical processes, SEM images of the obtained microstructure were taken for different growth rates (V) and the microstructure of the Zn–Al–Cu has fine lamellar eutectic and λ decreases with increasing V.
2. Effects of λ_E and V on ρ were determined in the form of Hall–Petch equation and logarithmic scale and the results obtained in the present work are found to be agree well with exist ρ values in literature for Zn-based alloys.
3. For the first time, the variation of K with V for the Zn–Al–Cu eutectic was measured with LHFM and the relationship between them in in the form of Hall–Petch equation and logarithmic scale were determined.

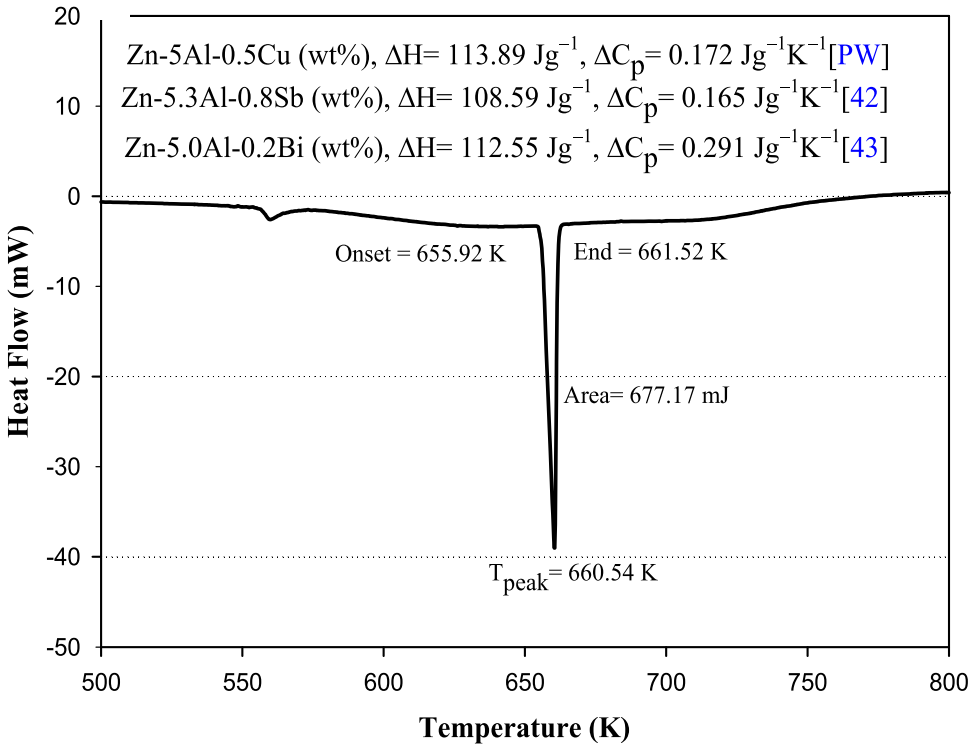

Fig. 7 Heat flow curve versus the temperature for Zn-5wt%Al-0.5wt%Cu eutectic alloy at a heating rate of 10 K min^{-1}

4. The highest and the smallest K values were obtained as 110.23 and 139.49 W K^{-1} m^{-1} with respect to the high growth rate of 8.458 μm s^{-1} and low growth rate of 2087.15 μm s^{-1}, respectively, at 300 K.
5. From DSC trace, ΔH and ΔC_P and T_M for Zn–5wt%Al–0.5wt%Cu eutectic alloy were found to be 113.89 J g^{-1}, 0.172 J g^{-1} K^{-1}, and 660.54 K, respectively.

Acknowledgements

The researchers are thankful to Erciyes University Scientific Research Project Unit for their financial supports under Contract Number: FDK-2013-4741.

References

1. Y. Zhang, K. Chu, S. He, B. Wang, W. Zhu, F. Ren, Mater. Sci. Eng. C. **106**, 110165 (2020)
2. L. Li, M. Zhao, L. Dong, D. Li, Surf. Coat. Technol. **394**, 125870 (2020)
3. X. Li, J. Liang, T. Shi, D. Yang, X. Chen, C. Zhang, Z. Liu, D. Liu, Q. Zhang, Ceram. Int. **46**, 12911–12920 (2020)
4. T. Wan, K. Chu, J. Fang, C. Zhong, Y. Zhang, X. Ge, Y. Ding, F. Ren, J. Mater. Sci. Technol. **80**, 266–278 (2021)
5. J.T. Krüger, K.P. Hoyer, V. Filor, S. Pramanik, M. Kietzmann, J. Meißner, M. Schaper, J. Alloys Compd. **871**, 159544 (2021)
6. I. Papageorgiou, C. Brown, R. Schins, S. Singh, R. Newson, S. Davis, J. Fisher, E. Ingham, C.P. Case, Biomaterials **28**, 2946–2958 (2007)
7. E. Guillamet, A. Creus, M. Farina, E. Sabbioni, S. Fortaner, R. Marcosa, Mutat. Res. **654**, 22–28 (2008)
8. D. Cadosch, E. Chan, O.P. Gautschi, L. Filgueira, J. Biomed. Mater. Res. A **91**, 1252–1262 (2009)
9. B. Scharf, C.C. Clement, V. Zolla, G. Perino, B. Yan, S.G. Elci, E. Purdue, S.R. Goldring, F. Macaluso, N. Cobelli, R.W. Vachet, L. Santambrogio, Sci. Rep. **4**, 5729 (2015)
10. G. Song, Corros. Sci. **49**, 1696–1701 (2007)
11. H. Wang, Z.M. Shi, K. Yang, Adv. Mater. Res. **32**, 207–210 (2008)
12. C.K. Seal, K. Vince, M.A. Hodgson, IOP Conf. Series **4**, 1 (2009)
13. C.W. Lin, C.P. Ju, J.H. Chern-Lin, Biomaterials **26**, 2899–2907 (2005)
14. V. Kumar, K.D. Gill, Arch. Toxicol. **83**, 965–978 (2009)

15. P.K. Bowen, J.-M. Seitz, R.J. Guillory, J.P. Braykovich, S. Zhao, J. Goldman, J.W. Drelich, J. Biomed. Mater. Res. B **106**, 245–258 (2018)
16. I.L.Z.R. Organization Engineering Properties of Zinc Alloys. International Lead Zinc Research Organization (1980)
17. E.M. da Costa, C.E. da Costa, F.D. Vecchia, C. Rick, M. Scherer, C.A. dos Santos, B.A. Dedavid, J. Alloys Compd. **488**, 89–99 (2009)
18. R. Caram, S. Milenkovic, J. Cryst. Growth 198–199; Part **I**, 844–849 (1999)
19. S.O. Adeosun, S.A. Balogun, L.O. Osoba, W.A. Ayoola, A.M. Oladoye, J. Mod. Manufact. Technol. **3**, 103–110 (2011)
20. D. Villegas-Cardenas, M.L. Saucedo-Muñoz, V.M. Lopez-Hirata, H.J. Dorantes-Rosales, J.L. Gonzalez-Velazquez, Mater. Res. **17**, 1137–1144 (2014)
21. X. Li, T. Shi, B. Li, X. Chen, C. Zhang, Z. Guo, Q. Zhang, Mater. Des. **183**, 108152 (2019)
22. X. Ren, H. Fu, J. Xing, Y. Yi, Mater. Sci. Eng. A **742**, 617–627 (2019)
23. E.A. Eid, E.H. El-Khawas, A.S. Abd-Elrahman, J. Mater. Sci: Mater. Electron. **30**, 6507–6518 (2019)
24. Y. Yokota, S. Horii, H. Ogino, M. Ogino, A. Yoshino, Y. Yamaji, S. Ohashi, K. Kurosawa, A.Y. Kamada, J. Electron. Mater. **48**, 1827–1832 (2019)
25. N. Ramesh Babu, M.R. Ramesh, S. Kiran Aithal, SILICON **12**, 701–713 (2020)
26. W. Yang, D.D.L. Chung, J. Mater. Sci: Mater. Electron. **32**, 7867–7874 (2021)
27. D.A. Porter, K.E. Easterlirng, M.Y. Sherif, *Phase Transformations in Metals and Alloys*, 3rd edn. (CRC Press, New York, 1992), pp. 189–229
28. H.Z. Fu, L. Liu, Mat. Sci. Forum **475–479**, 607–612 (2005)
29. A.E. Ares, L.M. Gassa, C.M. Mendez, Corrosion Resistance of Directionally Solidified Casting Zinc–Aluminium Matrix, Ed Dr. Shih (2012)
30. M. Rhême, F. Gonzales, M. Rappaz, Scr. Mater. **59**, 440–443 (2008)
31. F. Gonzales, M. Rappaz, Metall. Mater. Trans. A **37**, 2797–2806 (2006)
32. C. Zhang, Y. Wu, M. Fang, S. Wu, X. We, Y. Cheng, Y. Sun, Chin. Sci. Bull. **42**, 2067–2072 (1997)
33. K.A. Jackson, J.D. Hunt, Trans. Metall. Soc. AIME **236**, 1129–1142 (1966)
34. R.M. Jordan, J.D. Hunt, Metall. Trans. A **2**, 3401–3410 (1971)
35. R. Seetharaman, Trivedi. Metall. Trans. A **19**, 2955–2964 (1988)
36. J.J. Favier, J. De Goer, Directional Solidification of Eutectic Alloys. European Space Agency Special Publications ESA SP-222 Paris, 127-128 (1984)
37. V.T. Witusiewicz, U. Hecht, S. Rex, M. Apel, Acta Mater. **53**, 3663–3669 (2005)
38. H. Kaya, E. Çadırlı, M. Gündüz, J. Mat, Process Technol. **183**, 310–320 (2007)
39. H. Kaya, E. Çadırlı, M. Gündüz, J. Mater. Eng. Perf. **12**, 456–469 (2003)
40. S. Engin, U. Böyük, H. Kaya, N. Maraşlı, Int. J. Min. Metal. Mater. **18**, 659–664 (2011)
41. E. Çadırlı, M. Şahin, J. Mater. Sci. **46**, 1414–1423 (2011)
42. Ü. Bayram, Y. Karamazı, P. Ata, S. Aksöz, K. Keşlioğlu, N. Maraşlı, Int. J. Mater. Res. **107**, 1005–1015 (2016)
43. Y. Karamazı, Ü. Bayram, P. Ata, S. Aksöz, K. Keşlioğlu, N. Maraşlı, Trans. Nonferrous Met. Soc. China **26**, 2320–2335 (2016)
44. Ü. Bayram, Investigation of the dependence of mechanical, electrical and thermal properties with structure parameters on the growth rates in the controlled directionally solidified aluminium contained multiple eutectic alloys, D. Ph. Thesis Erciyes University Kayseri-Turkey (2017)
45. Y. Ocak, S. Aksöz, N. Maraşlı, E. Çadırlı, Fluid Pha. Equil. **295**, 60–67 (2010)
46. S. Aksöz, Y. Ocak, N. Maraşlı, K. Keşlioğlu, Exp. Ther. Fluid Sci. **35**, 395–404 (2011)
47. E. Öztürk, S. Aksöz, K. Keşlioğlu, N. Maraşlı, Therm. Acta **554**, 63–70 (2013)
48. Ü. Bayram, N. Maraşlı, J. Alloys Compd. **753**, 695–702 (2018)
49. V. Rudnev, D. Loveless, R. Cook, M. Black, *Handbook of Induction Heating* (Markel Dekker Inc., New York, 2003)
50. L.B. Valdes, Proc. IRE. **42**, 420–427 (1954)
51. H. Kaya, U. Böyük, S. Engin, E. Çadırlı, N. Maraşlı, J. Electron. Mater. **39**, 303–311 (2010)
52. E. Çadırlı, U. Böyük, H. Kaya, N. Maraşlı, S. Aksöz, Y. Ocak, J. Electron. Mater. **40**, 195–200 (2011)
53. J.B. Biot, Traite de Physique. Paris **4**, 669 (1816)
54. J.B.J. Fourier, *The Analytical Theory of Heat* (Dover Publication, New York, 1955)
55. S. Aksöz, E. Öztürk, N. Maraşlı, Measurement **46**, 161–170 (2013)
56. N. Aksöz, E. Öztürk, Ü. Bayram, S. Aksöz, S. Kervan, A. Ülgen, N. Maraşlı, J. Electron. Mater. **42**, 3573–3581 (2013)
57. Materials Science International Team, Light Metal Systems, Part 2 Volume 11A2, of the series Landolt–Börnstein–Group IV Physical Chemistry Aluminium–Copper–Zinc. pp. 182–205 (2003)
58. V.S. Zolotorevsky, N.A. Belov, M.V. Glazoff, *Casting Aluminium Alloys* (Elsevier, Pittsburgh, 2007), pp. 34–35

59. G.T. Meaden, Electrical Resistance of Metals, International Cryogenics Monograph Series, Chapter 1, Springer Science, France, LLC (1965)
60. Y.S. Touloukian, R.W. Powell, C.Y. Ho, P.G. Klemensi, *Thermal Conductivity Metallic Elements and Alloys*, vol. 1 (IFI, New York, 1970), pp. 1–10
61. Y.S. Touloukian, R.W. Powell, C.Y. Ho, P.G. Klemen, *Thermal Conductivity Metallic Elements and Alloys*, vol. 1 (IFI, New York, 1970), pp. 450–460
62. Y.S. Touloukian, R.W. Powell, C.Y. Ho, P.G. Klemensi, *Thermal Conductivity Metallic Elements and Alloys*, vol. 1 (IFI, New York, 1970), pp. 25–40
63. S. Aksöz, Y. Ocak, N. Maraşlı, K. Keşlioğlu, Fluid Phase Equilib. **293**, 32–41 (2010)